[redacted]

Copy 18
NASA TM X-97

NASA TM X-97

[redacted]

TECHNICAL MEMORANDUM

X-97

EFFECTS OF NOZZLE-SHROUD MISALINEMENT ON PERFORMANCE OF A FIXED-SHROUD DIVERGENT EJECTOR

By Andrew J. Stofan

Lewis Research Center
Cleveland, Ohio

DECLASSIFIED
NASA CLASS. CHANGE NOTICE
Issue No. 214
Date 8-11-71

CLASSIFIED DOCUMENT - TITLE UNCLASSIFIED

NATIONAL AERONAUTICS AND SPACE ADMINISTRATION
WASHINGTON March 1960

[redacted]

E-526

ERRATA

NASA TECHNICAL MEMORANDUM X-97

By Andrew J. Stofan

March 1960

Abstract: Lines 10 to 12 should read "gap at the bottom than at the top; the ratio of the gap at the bottom divided by the gap at the top was varied from 1.0 to 1.98."

Page 2, paragraph 1: Lines 6 to 9 should read "by holding the primary nozzle fixed and lowering the shroud; this resulted in a larger gap at the bottom than at the top between the nozzle and the shroud. The gap-height ratio (gap height at bottom divided by gap height at top) was varied from 1.0 to 1.98."

Page 13: Figure 5 should be replaced by the following figure:

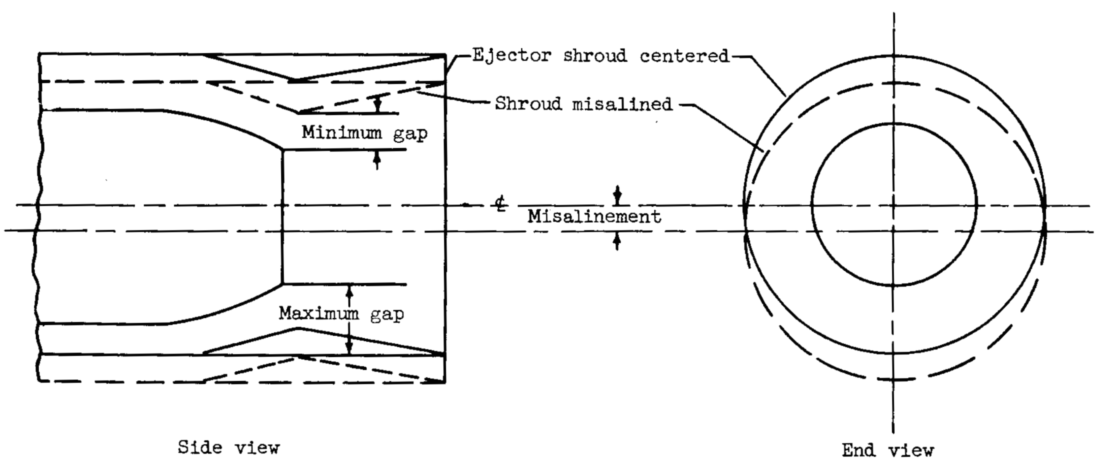

Figure 5. - Nozzle misalinement, gap-height ratio (max. gap/min. gap).

E-526

NATIONAL AERONAUTICS AND SPACE ADMINISTRATION

TECHNICAL MEMORANDUM X-97

EFFECTS OF NOZZLE-SHROUD MISALINEMENT ON PERFORMANCE OF A FIXED-SHROUD DIVERGENT EJECTOR*

By Andrew J. Stofan

SUMMARY

An investigation was conducted on a fixed-shroud divergent ejector, applicable to a Mach 2 aircraft, with a two-position primary nozzle to ascertain whether or not transverse misalinement of the primary nozzle with respect to the shroud would introduce unwanted side forces of appreciable magnitude. The two-position primary nozzle simulated a nonafterburning and an afterburning operating condition. In the course of the investigation, the effects of misalinement on ejector performance were also evaluated.

In general, the vertical forces caused by the misalinement were negligible when the ejector was operated at, or near, design conditions. However, when the ejector was operated at off-design conditions corresponding to those that would be encountered when the aircraft would be accelerating with afterburning through the high-subsonic Mach number region, the vertical force became as high as 4.7 percent of the axial thrust. Misalinement had little or no effect on either the axial-thrust performance or the pumping characteristics of the ejector.

CN-1

INTRODUCTION

Mach 2 turbojet aircraft equipped with afterburner sometimes employ fixed-shroud divergent ejectors because of the simplification and weight saving that are afforded; however, these attributes must offset the loss in thrust performance at off-design conditions (ref. 1). In some installations, the primary nozzle and the shroud are independently mounted, the nozzle to the engine and the shroud to the airframe. In such cases, it is possible that during flight sufficient transverse misalinement can occur between nozzle and shroud, as a result of thermal and pressure forces, to produce unwanted side forces. The possibility of this was evidenced during a recent small-scale ejector performance investigation

*Title, Unclassified.

and also in flight tests of a prototype, high Mach number airplane equipped with a fixed-shroud ejector. In the ejector investigation, slight misalinement of the primary nozzle and shroud caused an unsymmetrical pressure distribution in the shroud that resulted in an unwanted side force. In the prototype airplane, a pitching force that was attributed to misalinement was encountered. In order to better evaluate the magnitude of this effect, a small-scale investigation was conducted in which the effects of transverse misalinement on axial thrust and side forces were systematically determined.

The present investigation, which included a fixed-shroud ejector with simulated nonafterburning and afterburning primary nozzles, was conducted in a cold-air test facility that was operated over a range of nozzle pressure ratios from 2 to 16. The secondary- to primary-flow ratio was varied from 0 to 0.08. The transverse misalinement was accomplished by holding the shroud fixed and lowering the primary nozzle; this resulted in a larger gap at the top than at the bottom between the nozzle and shroud. The gap-height ratio (gap height at top divided by gap height at bottom) was varied from 1.0 to 1.98.

E-526

APPARATUS AND INSTRUMENTATION

The fixed-shroud divergent ejector with simulated nonafterburning and afterburning primary nozzles, illustrated in figure 1, was modeled after that of a prototype Mach 2.2 aircraft. The nonafterburning and afterburning configurations had geometric expansion ratios of 3.38 and 1.96, respectively.

The installation of the ejector configurations in the testing facility is shown in figures 2 and 3. The ejectors were fastened to the mounting pipe, which was in turn attached to a bedplate freely suspended from four flexure rods, and this entire assembly was installed in a plenum chamber. High-pressure air was supplied to the nozzle by the laboratory air-supply system, and the plenum chamber was exhausted to the laboratory exhaust system. Pressure difference across the nozzle was made possible by labyrinth seals installed around the mounting pipe. Two vent lines between the two labyrinth seals and the plenum chamber decreased the pressure differential across the second labyrinth seal and prevented dynamic pressures from acting on the outside of the diffuser section. Forces acting on the nozzle and mounting pipe, both external and internal, were transmitted from the bedplate through a flexure-supported bell crank and linkage to a balanced, air-pressure-diaphragm, force-measuring cell. This entire system, which includes inlet pipe, labyrinth seals, secondary-hose connection, air-measuring station, and thrust-measuring cell, was calibrated before the ejectors were installed. For a more detailed explanation of the testing facility, see reference 2.

INSTRUMENTATION

Pressures and temperatures were measured at various stations as shown in the following table and in figure 2.

Station	Total-pressure tubes	Static-pressure taps	Temperature thermocouples
0 - Exhaust	-	4	-
1 - Mounting-pipe inlet	-	4	2
2 - Airflow	12	8	-
3 - Primary-nozzle inlet	8	4	2
4 - Secondary-air passage	12	-	-
Secondary-air orifice	-	2	2

Pressures obtained from total-pressure rakes and wall static taps at stations 1 and 2 were used in the computation of inlet momentum and airflow, respectively. Total-pressure and total-temperature rakes were installed at station 3 to determine nozzle-inlet conditions and at station 4 to measure secondary total pressure. Station 0 was used to measure plenum-chamber static pressure and temperature. The secondary flow was measured by a flat-plate orifice, two static-pressure taps, and two thermocouples located in the secondary-air line.

Static-pressure taps set on equal areas on the top and bottom of the ejector shroud were used to determine the forces in the vertical plane. The location of these taps is shown in figure 4.

PROCEDURE

The testing procedure was the same for both the nonafterburning and afterburning configurations. For each combination of gap-height ratio (see fig. 5 for explanation of gap-height ratio) and secondary-weight-flow ratio w_s/w_p indicated in the following table, the nozzle pressure ratio P_p/p_0 was varied over a range of approximately 2 to 16. The ranges of gap-height ratios investigated were selected on the basis of some unpublished full-scale information which indicated that gap-height ratios of as much as 1.16 for the nonafterburning configuration and 1.40 for the afterburning configuration are possible.

Configuration	Gap-height ratio	Secondary-flow ratio
Nonafterburning	1.0 1.16 1.24	0, 0.02, 0.08
Afterburning	1.0 1.40 1.98	0, 0.015, 0.07

The symbols used and the calculation of the forces in the vertical plane (by a pressure-area integration) are shown in appendixes A and B, respectively. The measured axial thrust was determined by summing up all the forces, both external and internal, that were acting on the nozzle - mounting-pipe system. The ideal thrust was calculated from the measured primary and secondary mass flows, with isentropic expansion assumed from the respective measured total pressure to ambient. The thrust ratio is the measured axial thrust divided by the ideal thrust.

RESULTS AND DISCUSSION

The axial thrust and the pumping performance for the nonafterburning and the afterburning configurations are shown in figures 6 to 9. These figures clearly show that the ranges of gap-height ratio covered had no effect on either the thrust ratio or the pumping characteristics of the ejectors. The dash lines in figure 6 indicate hysteresis effects, and, as can be seen, these effects are unchanged by the variation in gap-height ratio.

The effects of gap-height ratio on the vertical-force ratio (vertical force over axial nozzle thrust) for the nonafterburning configuration at secondary-flow ratios of 0 and 0.02 are shown in figure 10. The data in the figures plus one data point at a w_s/w_p of 0.08 and a gap-height ratio of 1.16 indicate that for the nonafterburning configuration the effect is negligible (less than 0.01). A vertical-force ratio of about 0.005 was measured at a gap-height ratio of 1.0 for both the nonafterburning and afterburning configurations. Although reasons for this are unknown, the effect is so small as to be considered negligible.

The effects of gap-height ratio on the vertical-force ratio for the afterburning configuration at secondary-flow ratios of 0, 0.015, and 0.07 are shown in figure 11. The effects are negligible (less than 0.01) except for low nozzle pressure ratios ($P_p/p_o = 3$) when operating at 0 and 0.07 secondary-flow ratios. The vertical-force ratios for w_s/w_p of 0 and 0.07 were 0.018 and -0.048, respectively. The zero weight-flow-ratio condition is not of practical importance because airplanes do not normally operate at this condition (especially with afterburning). When the aircraft would be accelerating through the high-subsonic Mach number region, however, a P_p/p_o of 3 and a w_s/w_p of 0.07 (or secondary-flow ratios in this region) would frequently be encountered.

The pressure profiles in the ejector shroud for the afterburning configuration at a nozzle pressure ratio of 3 and a gap-height ratio of 1.98 are shown in figure 12. As would be expected, these profiles indicate that, for the secondary-flow ratios examined, the flow is overexpanded. For a w_s/w_p of 0 and 0.015, the overexpansion is essentially symmetrical with pressure, only slightly different on the top of the shroud than on the bottom. For a w_s/w_p of 0.07, however, the primary flow appears to have detached from the bottom of the shroud but not from the top; this results in a relatively uniform pressure along the bottom that is considerably higher than the pressure along the top. The result was that the largest vertical-force ratio was obtained at these conditions.

SUMMARY OF RESULTS

The results of an investigation conducted on a small-scale fixed-shroud divergent ejector with a two-position primary nozzle (simulating a nonafterburning and an afterburning configuration) to determine whether or not transverse misalinement of the primary nozzle with respect to the shroud would introduce unwanted side forces indicated that:

1. The only condition where the vertical-force ratio became appreciable was with the afterburning configuration at a nozzle pressure ratio of 3, a secondary-flow ratio of 0.07, and a gap-height ratio of 1.98. This would correspond to the off-design condition of acceleration with afterburning through the high-subsonic Mach number region.

2. The variation of gap-height ratio had no effects on the axial-thrust ratio or on the pumping performance of the ejectors.

Lewis Research Center
National Aeronautics and Space Administration
Cleveland, Ohio, July 22, 1959

APPENDIX A

SYMBOLS

The following symbols are used in this report:

A	area, sq ft
F	actual thrust
F_i	ideal thrust
l	axial length measured along ejector shroud
P	total pressure, lb/sq ft
p	static pressure, lb/sq ft
r	radius of ejector
w	airflow, lb/sec

Subscripts:

e	ejector exit
max	maximum
o	exhaust
p	primary
s	secondary
v	vertical
1	mounting-pipe-inlet station
2	airflow measuring station
3	primary-nozzle-inlet station
4	secondary-air-passage station

E-526

APPENDIX B

VERTICAL-FORCE COMPUTATION

The ejector shroud was divided into six axial segments, and the force in the vertical direction for each segment was found. Then, all the segment forces were summed up to give a net vertical force.

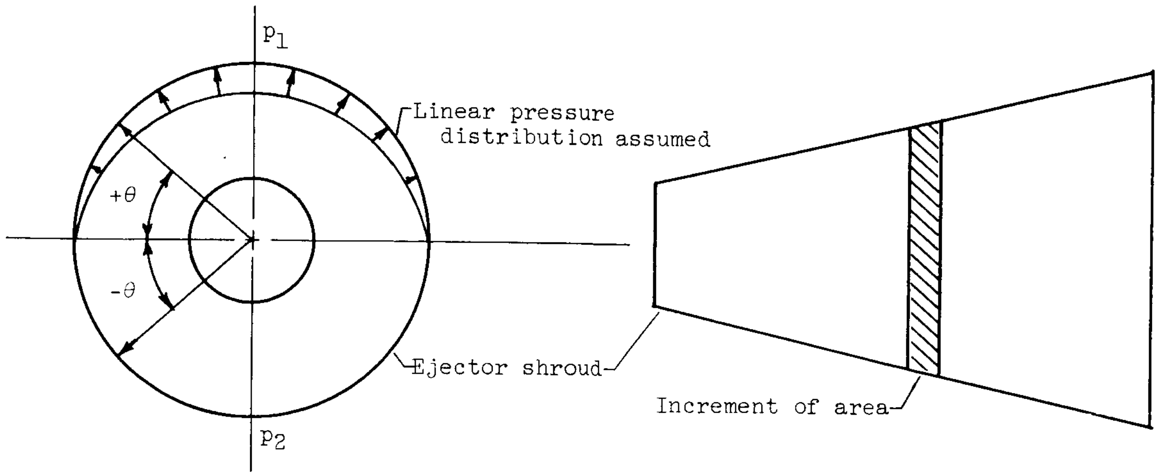

End view

Side view

The p_1 and p_2 values were measured by static-pressure taps. As seen in figure 4, there were also some static-pressure taps on the shroud, spaced halfway between the top and bottom rows, which indicated pressures halfway between p_1 and p_2. A linear variation of pressure difference ($\Delta p = (p_1 - p_2)$) with angle θ was therefore assumed (p_1 measured at $+\theta$, p_2 at $-\theta$). The maximum pressure difference Δp_{max} thus occurred at 90°.

$$\Delta p = \theta/\tfrac{\pi}{2}\, \Delta p_{max} \qquad (0^\circ \geq \theta \leq 90^\circ)$$

The force F acting on an increment of area dA is

$$F = \int \Delta p \, dA$$

The vertical component of this force is

$$F_V = \int \Delta p \, dA \sin \theta$$

Since $\Delta p = \theta/\frac{\pi}{2} \, \Delta p_{max}$,

$$F_V = \int_0^{\pi/2} \frac{\theta}{\pi/2} \Delta p_{max} \, dA \sin \theta$$

Since $dA = r \, d\theta \, l$,

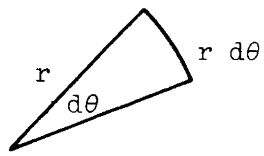

r, radius of shroud

l, axial length along ejector shroud

$$F_V = \int_0^{\pi/2} \theta/\tfrac{\pi}{2} \, \Delta p_{max} \, r \, d\theta \, l \sin \theta$$

$$= \frac{2rl \, \Delta p_{max}}{\pi} \int_0^{\pi/2} \theta \sin \theta \, d\theta$$

$$= \frac{2rl \, \Delta p_{max}}{\pi} (\sin \theta - \theta \cos \theta)_0^{\pi/2}$$

$$= \frac{2rl \, \Delta p_{max}}{\pi} (1) = 0.63661 \, rl \, \Delta p_{max}$$

To get the net vertical force (from $0 \rightarrow \pi$), multiply by 2:

$$F_V = 1.27322 \, rl \, \Delta p_{max}$$

The effect of shroud divergence is:

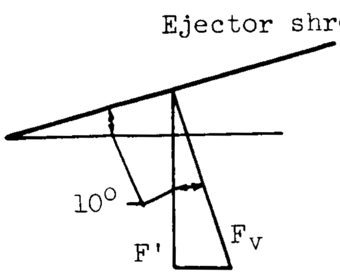

F' = net force acting in vertical plane on one segment of area

$F_V = 1.27322 \, rl \, \Delta p_{max}$

$F' = F \cos 10^\circ = (1.27322 \, rl \, \Delta p_{max}) \cos 10^\circ$

$F' = 1.2538 \, rl \, \Delta p_{max}$

The total vertical force acting on the shroud is the summation of all the forces acting on each segment:

$$F_{total} = \sum F'$$

E-526

REFERENCES

1. Beheim, Milton A.: Off-Design Performance of Divergent Ejectors. NACA RM E58G10a, 1958.

2. Trout, Arthur M., Papell, S. Stephen, and Povolny, John H.: Internal Performance of Several Divergent-Shroud Ejector Nozzles with High Divergence Angles. NACA RM E57F13, 1957.

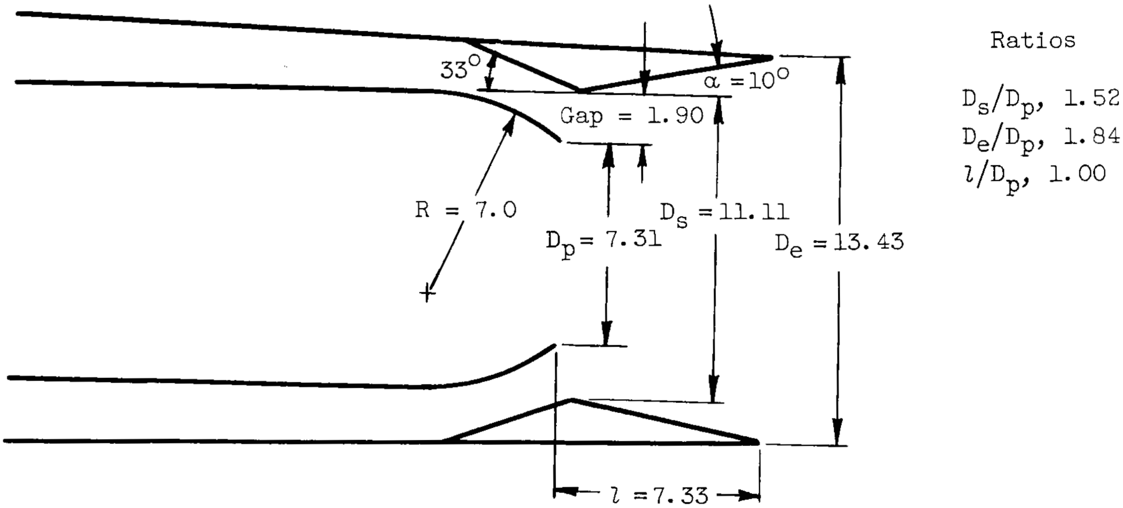

(a) Nonafterburning.

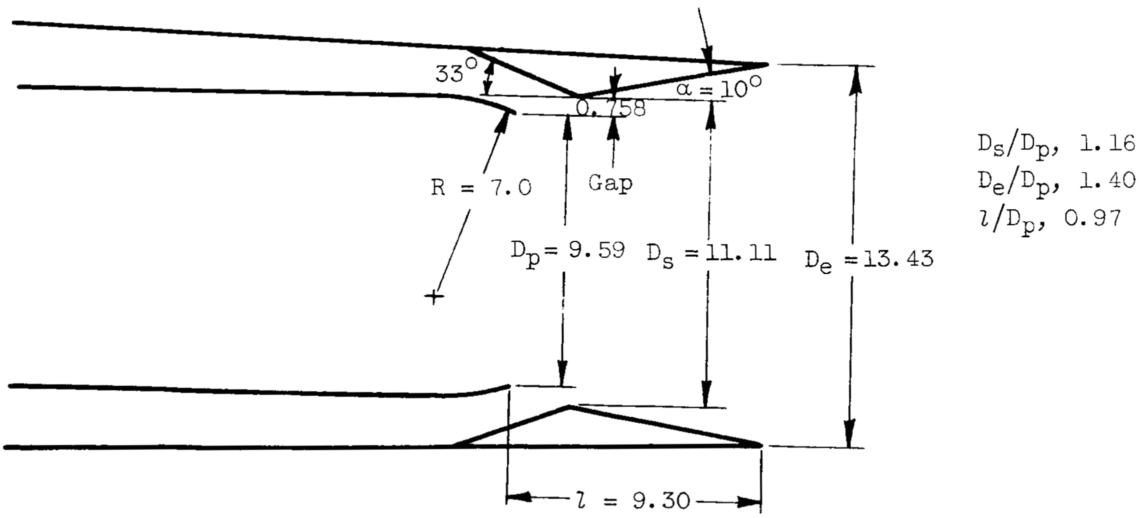

(b) Afterburning.

Figure 1. - Ejector nozzles before misalinement. (All dimensions in inches.)

E-526

CN-2 back

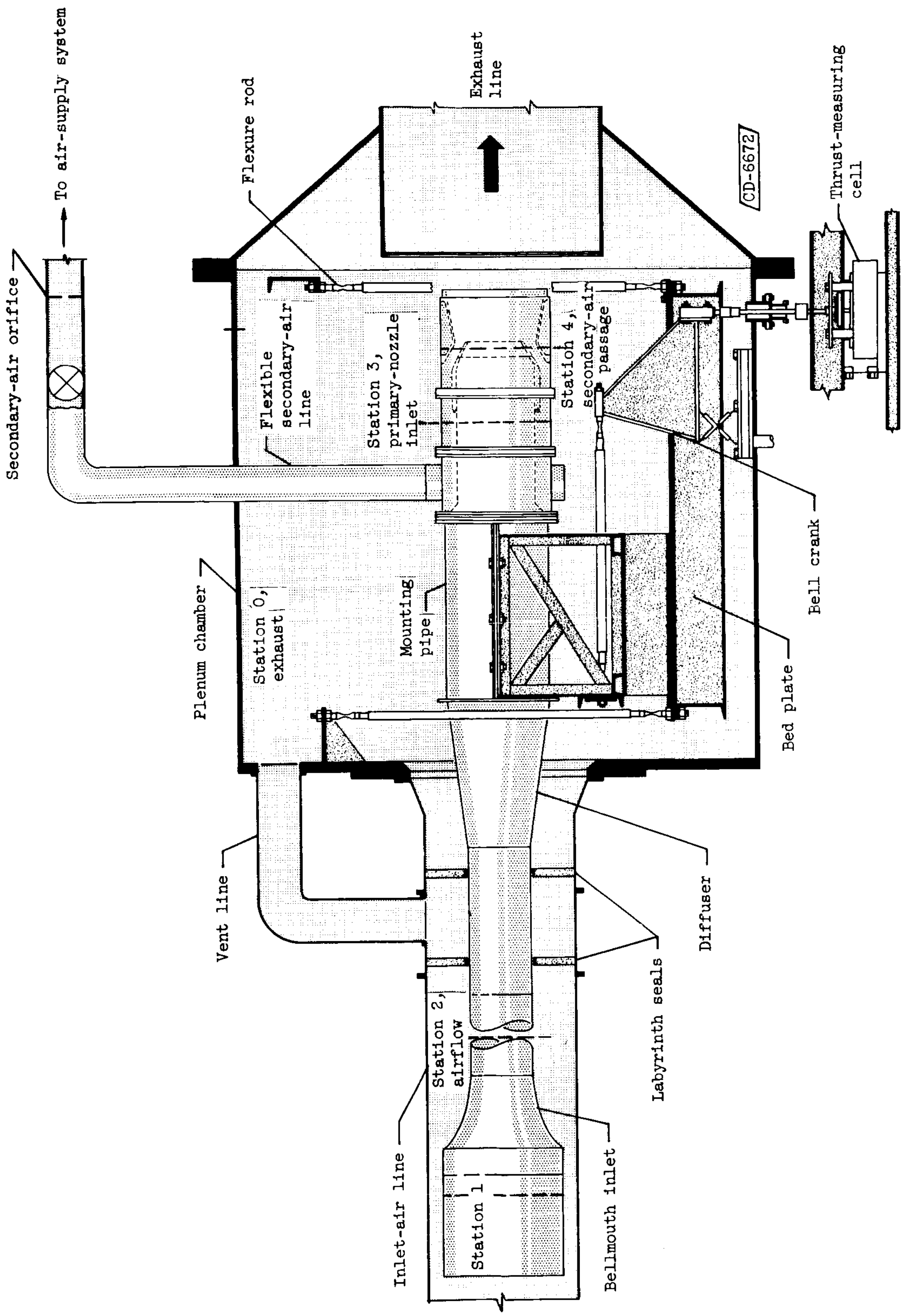

Figure 2. - Nozzle test facility.

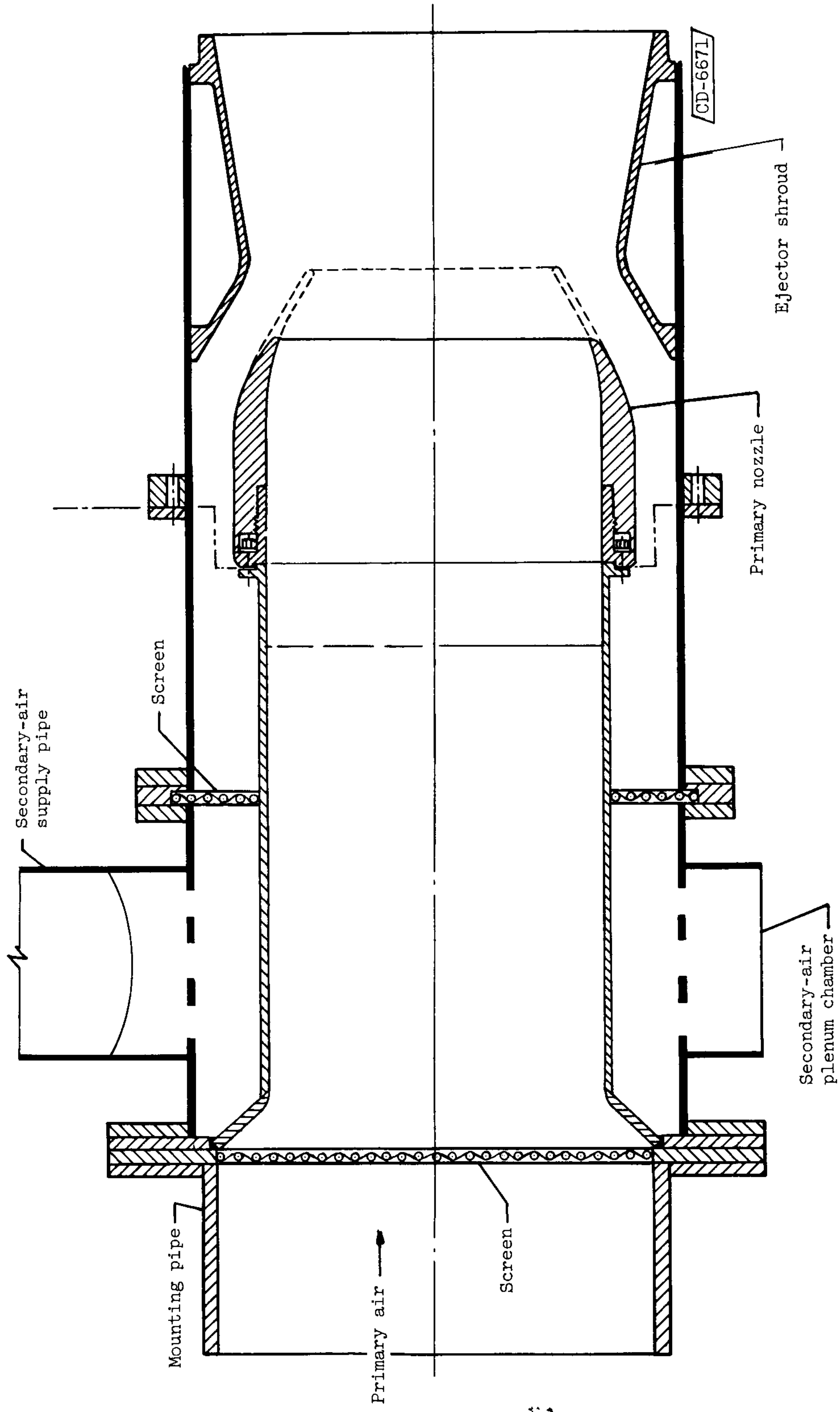

Figure 3. - Ejector installation.

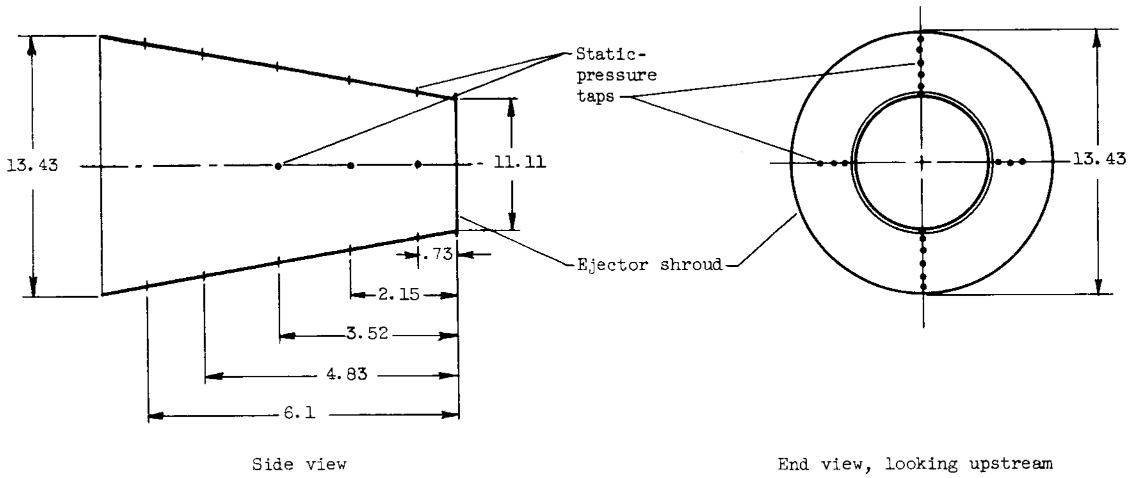

Figure 4. - Shroud instrumentation. (All dimensions in inches.)

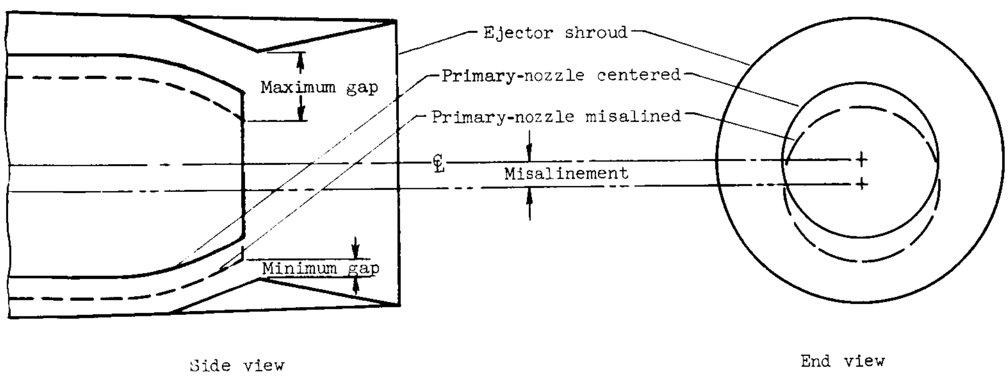

Figure 5. - Nozzle misalinement, gap-height ratio (max. gap/min. gap).

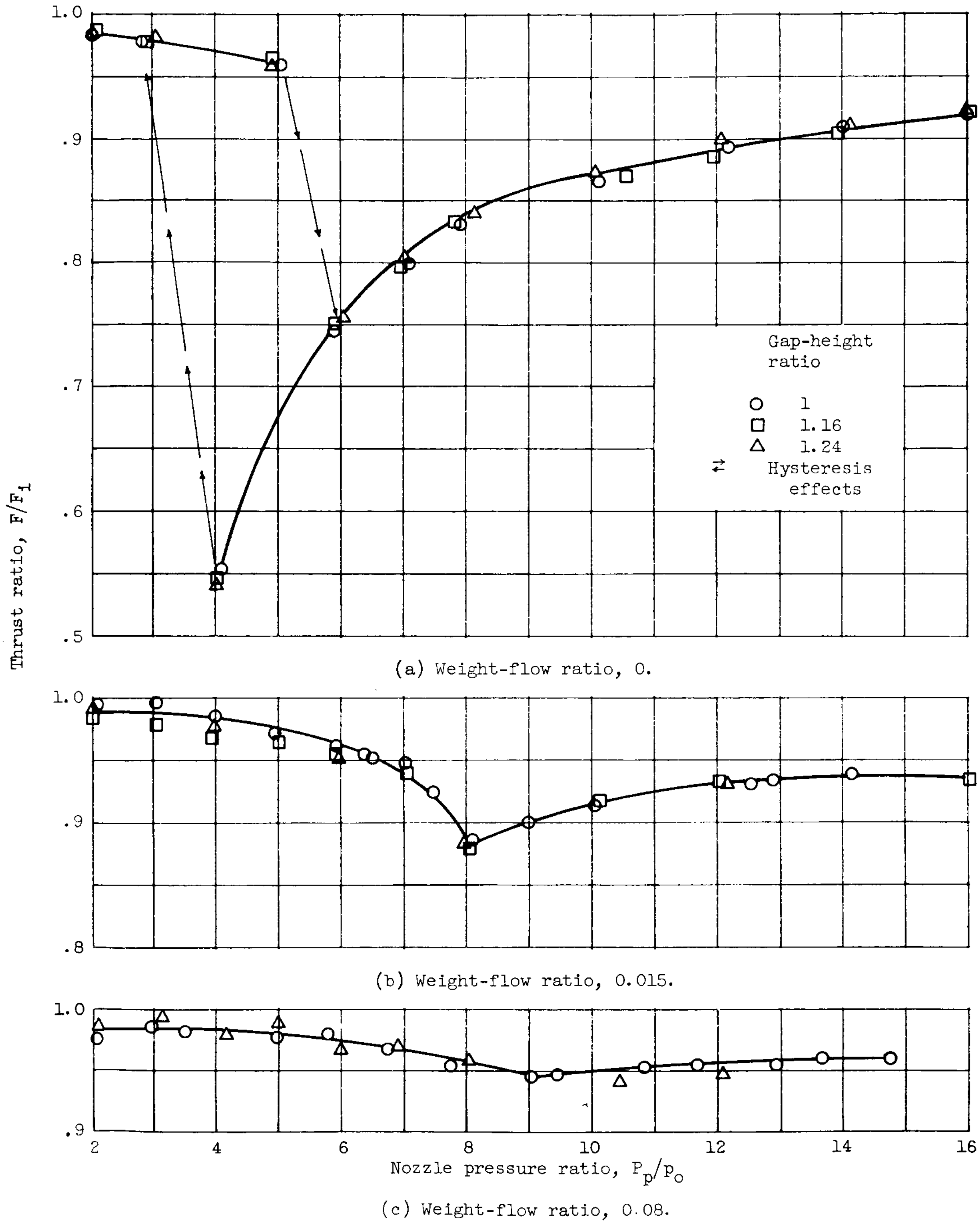

Figure 6. - Effect of gap-height ratio on thrust ratio for nonafterburning configuration.

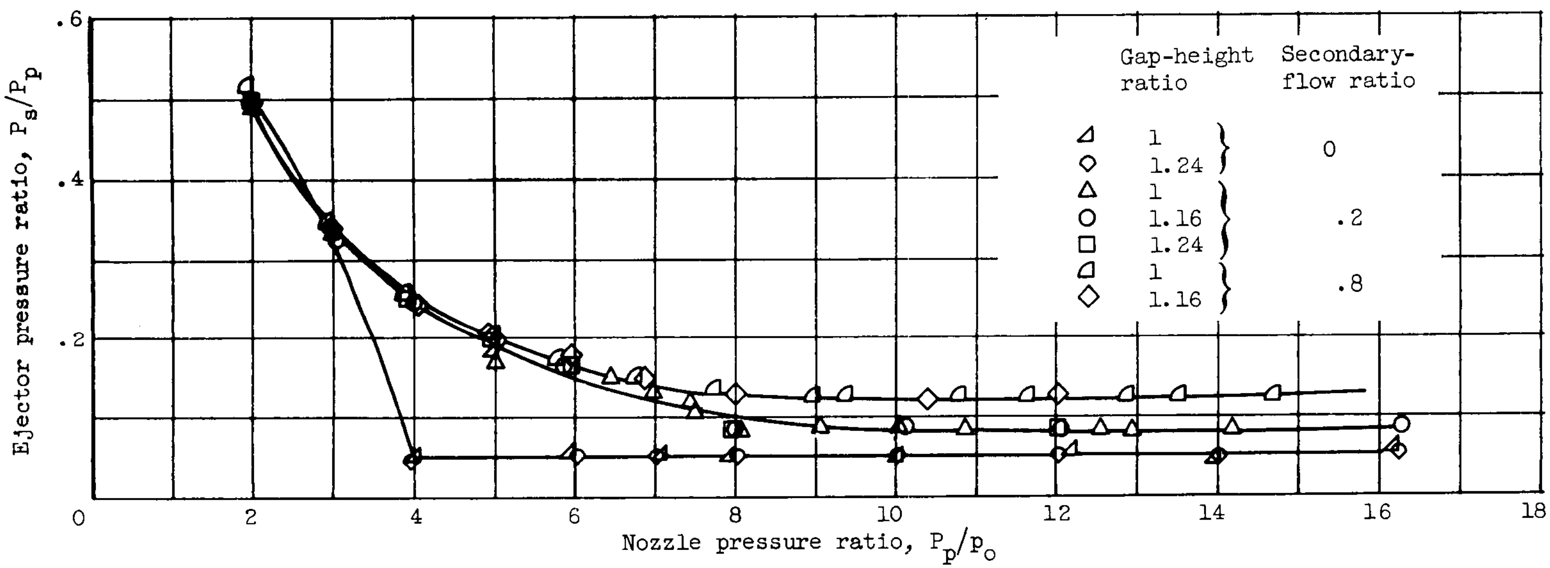

Figure 7. - Effect of gap-height ratio on pumping performance for nonafterburning configuration.

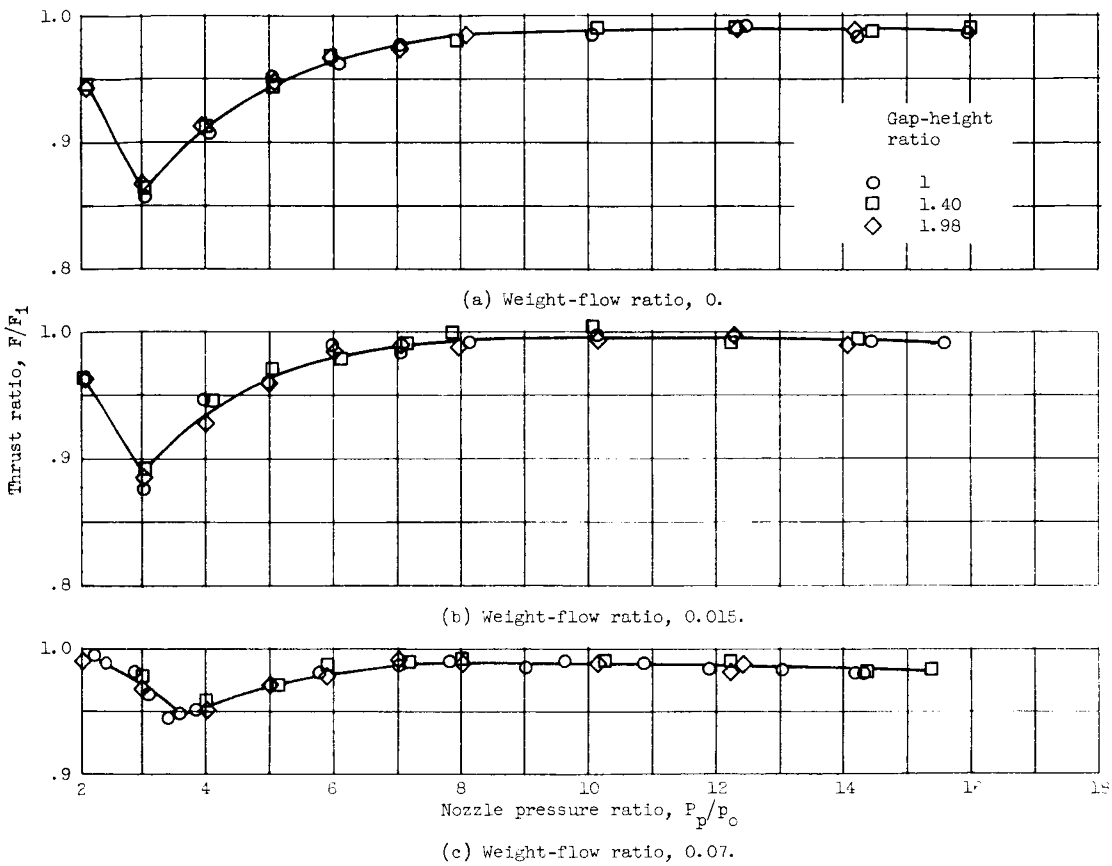

Figure 8. - Effect of gap-height ratio on thrust ratio for afterburning configuration.

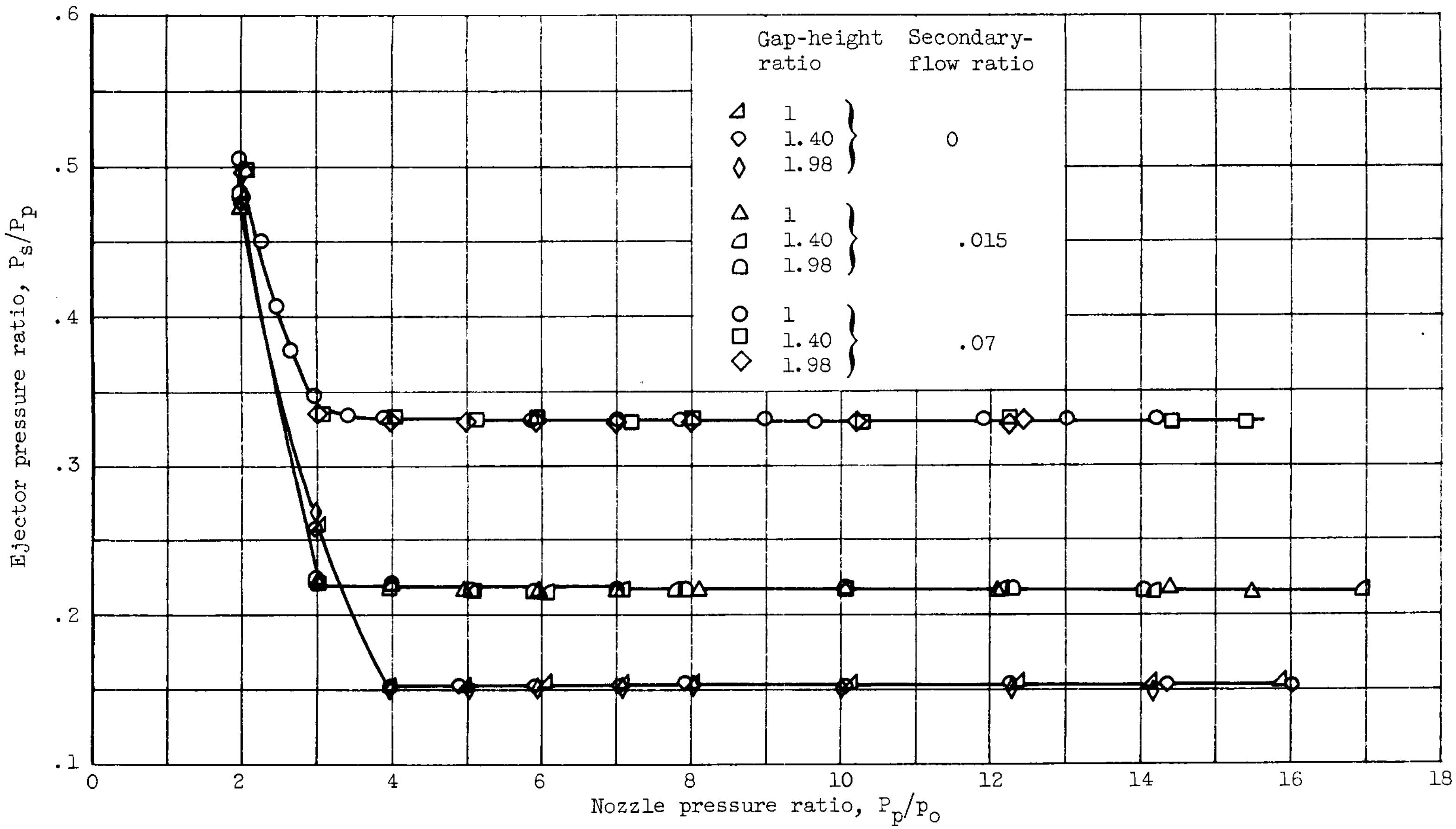

Figure 9. - Effect of gap-height ratio on pumping performance for afterburning configuration.

E-526

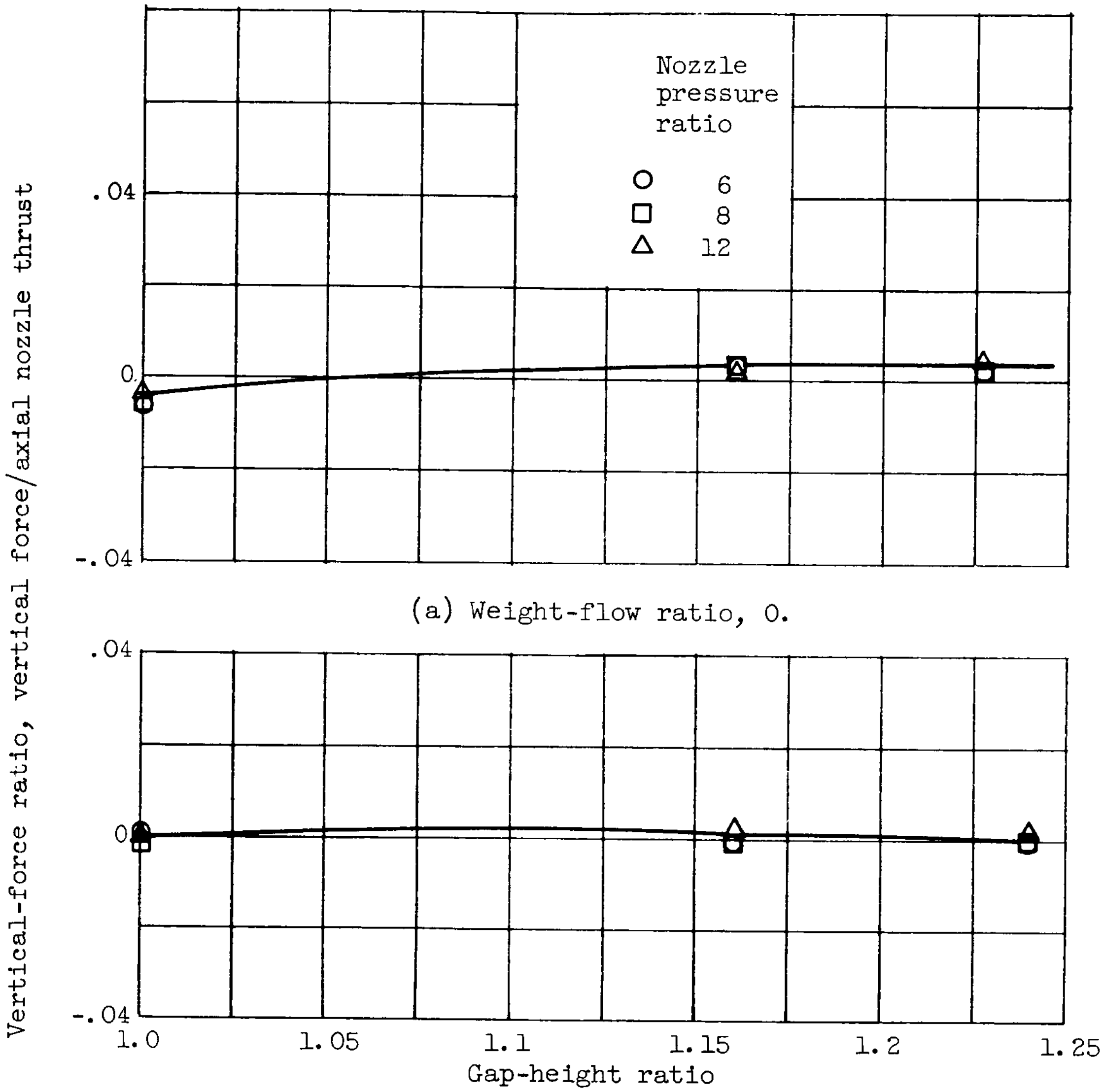

(a) Weight-flow ratio, 0.

(b) Weight-flow ratio, 0.02.

Figure 10. - Effect of gap-height ratio on vertical-force ratio for nonafterburning configuration.

E-526

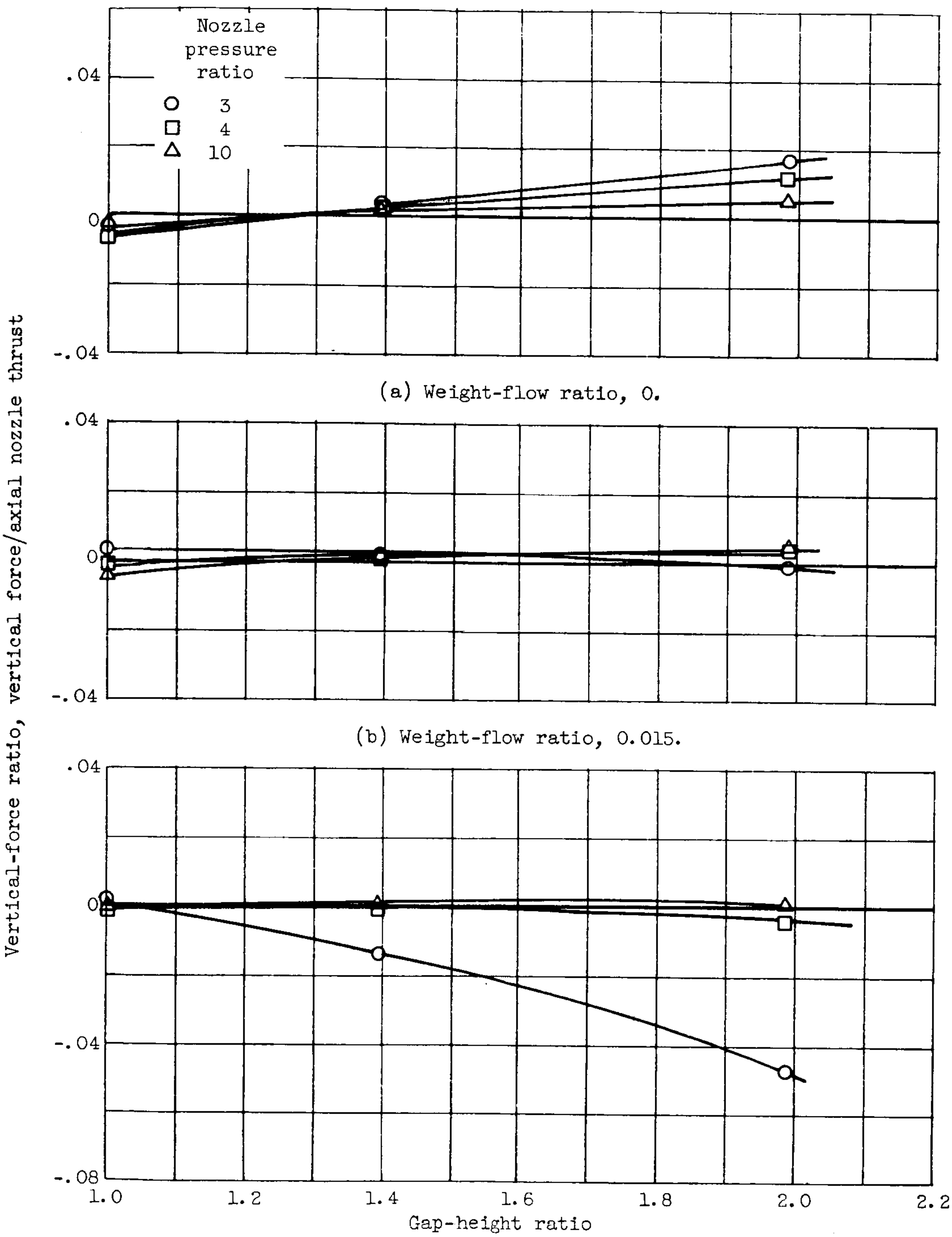

(a) Weight-flow ratio, 0.

(b) Weight-flow ratio, 0.015.

(c) Weight-flow ratio, 0.07.

Figure 11. - Effect of gap-height ratio on vertical-force ratio for afterburning configuration.

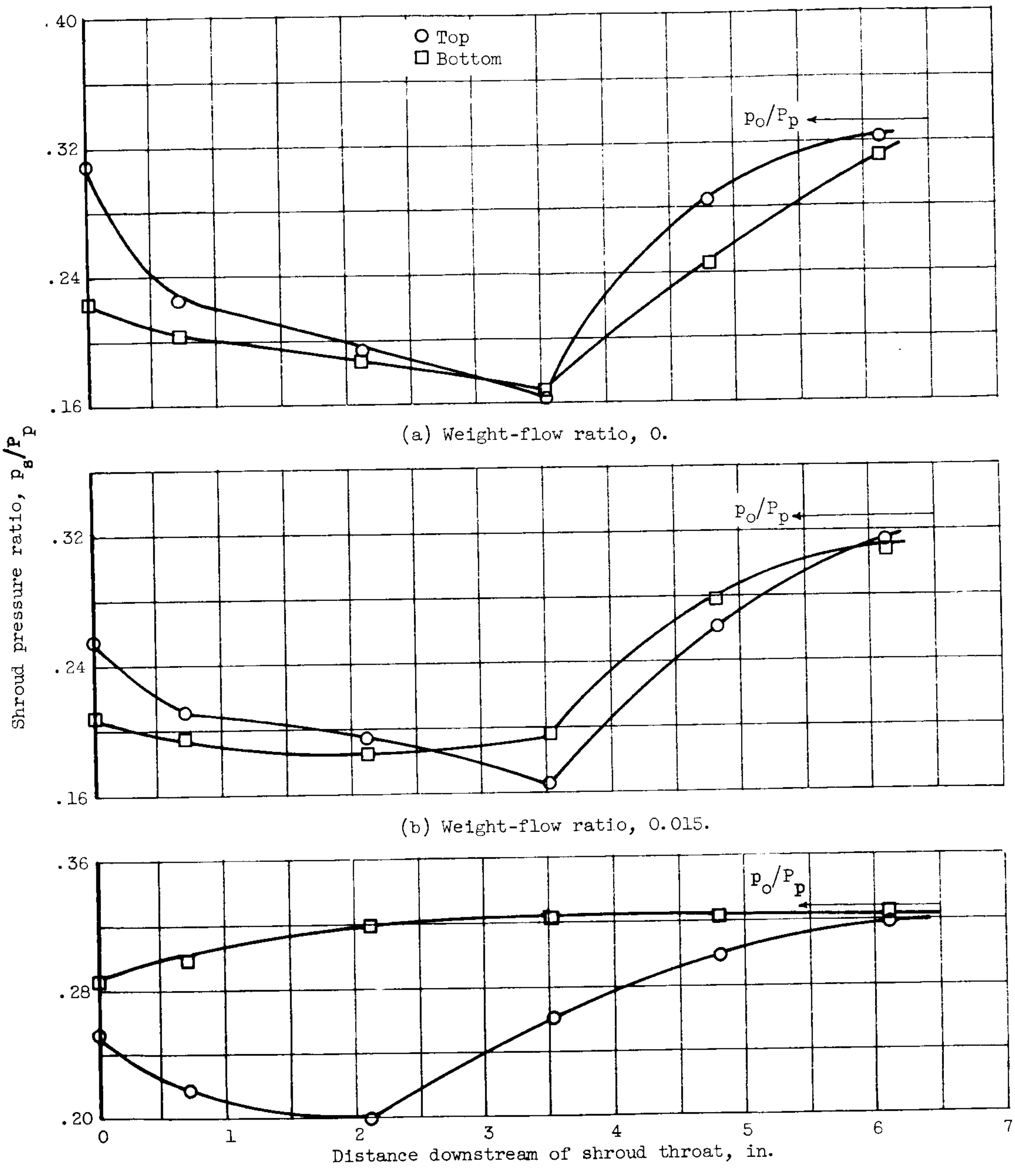

(c) Weight-flow ratio, 0.07.

Figure 12. - Effect of secondary-flow ratio on pressure distribution in shroud for afterburning configuration at a gap-height ratio of 1.98.